

Molecular Physics

An International Journal at the Interface Between Chemistry and Physics


ISSN: 0026-8976 (Print) 1362-3028 (Online) Journal homepage: <https://www.tandfonline.com/loi/tmph20>


Odd-even effect of the number of free valence electrons on the electronic structure properties of gold-thiolate clusters

Yanle Li, Chunyan Liu, Vytor Oliveira, Dieter Cremer, Zijia Chen & Jing Ma

To cite this article: Yanle Li, Chunyan Liu, Vytor Oliveira, Dieter Cremer, Zijia Chen & Jing Ma (2019) Odd-even effect of the number of free valence electrons on the electronic structure properties of gold-thiolate clusters, *Molecular Physics*, 117:9-12, 1442-1450, DOI: [10.1080/00268976.2018.1554864](https://doi.org/10.1080/00268976.2018.1554864)

To link to this article: <https://doi.org/10.1080/00268976.2018.1554864>

 View supplementary material 

 Published online: 05 Dec 2018.

 Submit your article to this journal 

 Article views: 23

 View Crossmark data 

Odd-even effect of the number of free valence electrons on the electronic structure properties of gold-thiolate clusters

Yanle Li^a, Chunyan Liu^b, Vytor Oliveira^c, Dieter Cremer^c, Zijia Chen^a and Jing Ma^a

^aKey Laboratory of Mesoscopic Chemistry of MOE, School of Chemistry and Chemical Engineering, Nanjing University, Nanjing, People's Republic of China; ^bCollege of Chemistry and Chemical Engineering, Hunan University, Changsha, People's Republic of China; ^cComputational and Theoretical Chemistry Group (CATCO), Department of Chemistry, Southern Methodist University, Dallas, TX, USA

ABSTRACT

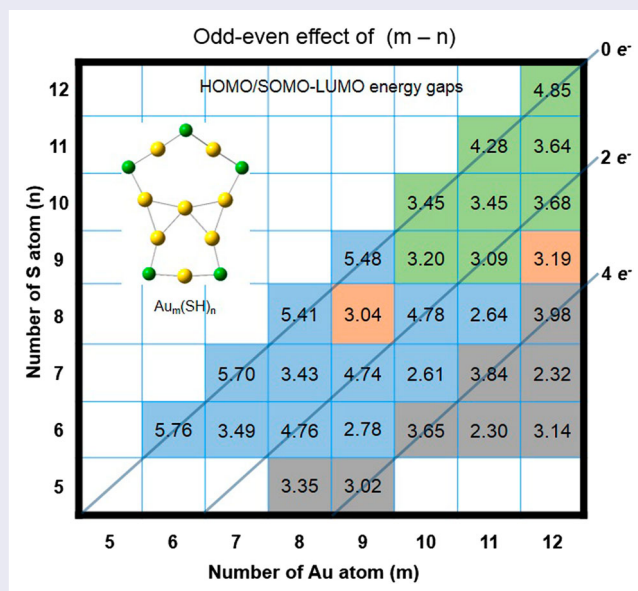
It is essential to understand the intrinsic stability of the gold-thiolate clusters, which present extensive potential applications in many fields such as the catalysis, biomedicines and molecular machines. The electronic structures and aromaticity indexes of a series of $Au_m(SH)_n$ ($m, n = 5-12$) were comprehensively investigated through energetic, vibrational, magnetic, and electronic density properties, which are highly sensitive to the size and topological structure of the cluster. Generally, computational results of energy gap between the frontier molecular orbitals, normalized atomization energy (NAE), and electron localization function (ELF)- σ values exhibit the odd-even effect, in which clusters with the even number of free valence electrons, being reflected by the value of $(m-n)$, possess relatively higher stability than the odd one. However, it is difficult to describe the stability of cluster with the sophisticated three-dimensional structure through one single aromaticity index such as the nucleus-independent chemical shift (NICS) value. Principal component analysis and clustering analysis of the calculation results of $Au_m(SR)_n$ clusters suggest that the value of $(m-n)$ and the Au_4 unit are important for predicting the stability of the Au clusters.





ARTICLE HISTORY


Received 14 August 2018
Accepted 27 November 2018

KEYWORDS

Gold-thiolate clusters; bond strength order; principal component analysis; clustering analysis



CONTACT Chunyan Liu  xigualiuchunyan@126.com  College of Chemistry and Chemical Engineering, Hunan University, Changsha, Hunan, People's Republic of China; Jing Ma  majing@nju.edu.cn  Key Laboratory of Mesoscopic Chemistry of MOE, School of Chemistry and Chemical Engineering, Nanjing University, Nanjing, Jiangsu, People's Republic of China

 Supplemental data for this article can be accessed here. <https://doi.org/10.1080/00268976.2018.1554864>

Introduction

The gold nanoclusters have aroused intensive interest since Haruta found that nanoscale Au exhibited excellent catalytic activity during CO oxidation in 1980s [1]. In addition to the application in catalysis, the extension to biomedicine and chemical sensing attracted tremendous attentions of both experimental and computational scientists [2–5]. The broad applications of Au nanomaterials correlate strongly with their thermodynamic stability. Therefore, many efforts have been made to figure out the relation between the geometry and stability of Au nanomaterial. In the recent decade, the progress on the precise synthesis of monodisperse thiolate-protected gold nanoclusters $\text{Au}_m(\text{SR})_n$ (denoted as RS-AuNPs), such as $\text{Au}_{24}(\text{SR})_{20}$, $\text{Au}_{25}(\text{SR})_{18}^-$ and $\text{Au}_{38}(\text{SR})_{24}$, etc. provided effective ways to explore catalytic processes and the size/geometrical effect of Au clusters in varied catalytic reactions [6–10]. Some groups have carried out extensive study on gold-thiolate clusters $\text{Au}_m(\text{SR})_n$ in our discussed size range ($m, n = 5\text{--}12$) with the 1:1 gold-to-thiolate ratio both theoretically and experimentally [11–17]. Additionally, some of the smallest gold-thiolate clusters that do not have a 1:1 ratio, such as $\text{Au}_{15}(\text{SCH}_3)_{13}$, have been investigated [18,19]. Based on the intrinsic rules concluded from these thiolate-protected Au nanoclusters, some structurally unresolved clusters have been predicted [20]. Theoretical study also played an important role. For instances, the ‘Divide and Protect’ structural rule was proposed in 2006, in which $\text{Au}_m(\text{SR})_n$ was divided as $\text{Au}_{m-n}(\text{AuSR})_n$ and considered as the high symmetric intact gold core covered by the outer ligands containing both Au as well as thiolate [21]. This was also supported by X-ray diffraction structures of the synthesised $\text{Au}_{102}(\text{SR})_{44}$ and $\text{Au}_{25}(\text{SR})_{18}^-$ [2,22].

With the precise experimental structure, vast theoretical work focused on revealing the relationship between the topological structures and electronic structures. Häkkinen and coworkers introduced superatom complex (SAC) model to explain high stability of several spherical-like ligand-protected gold clusters [23]. The clusters with free valence electron number equal to that of the noble-gas were presumed to have higher stability. However, the SAC model did not work well for the clusters with non-spherical core. Later, supervalence bond (SVB) model was proposed and the non-spherical bi-icosahedral Au_{23}^{9+} core of $\text{Au}_{38}(\text{SR})_{24}$ could be viewed as a superatomic molecule. The Au_{23}^{9+} core is an exact analogue of the covalent F_2 molecule from the molecular orbital aspect [24]. Cheng et al. [25] also developed the superatom-network (SAN) to study the chemical bonding of electronically stable compounds $\text{Au}_{18}(\text{SR})_{14}$, $\text{Au}_{20}(\text{SR})_{16}$, and $\text{Au}_{24}(\text{SR})_{20}$. Given that the

valence electrons of the above clusters disobeyed the electron counts rule of the SAC model, the chemical bonding of these gold cores was revised as a network of \mathbf{n} center-two electron, $\mathbf{nc}\text{-}2e$ ($\mathbf{n} = 2, 3, 4$) superatom. Recently, Gao and coworkers developed a grand unified model (GUM) to describe the stability of a series of RS-AuNPs through an important principle that Au cores of the different sized RS-AuNPs can be built through the combination of elementary blocks such as triangular $\text{Au}_3(2e)$ and tetrahedral $\text{Au}_4(2e)$ [26].

In addition, an emphasis was laid on the different size-evolution paths during the nucleation and growth processes to form stable $\text{Au}_m(\text{SR})_n$ clusters ($m, n = 5\text{--}12$), i.e. core growth with increasing m , core dissolution with increasing n , and staple-motif growth with simultaneously increasing m and n , respectively [27]. An obvious $2e^-$ growth rule and the important role of Au_4 building unit were also demonstrated in our previous work [27]. Recently, we also investigated the aromaticity of planar Au_m clusters without the thiolate ligands [28]. For the first time, we proposed that each planar Au_m cluster could be constructed from several 3-ring $\text{Au}_3(2e)$ building blocks [28]. With the increase of the number of shared edges between two neighbouring Au_3 units, the nucleus-independent chemical shift (NICS) values of Au_3 units decrease, so does the local ring aromaticity, which reminded us of the Clar’s rule for the polycyclic π -aromatic polybenzenoides [29], as well as inorganic BN analogues of polybenzenoid hydrocarbon systems [30]. Hence, we named this phenomenon as like-Clar’s rule to describe the dilution of the aromaticity of planar clusters upon ring fusing of $\text{Au}_3(2e)$ building units. The strength of an Au–Au bond of the Au_m clusters was also analyzed by local vibrational modes with the Konkoli-Cremer method to determine a bond strength order (BSO) [31–33]. A simple building principle for small Au_m clusters from $\text{Au}_3^+(2e)$ and $\text{Au}_3(3e)$ subsystems, was predicted by their vibrational properties in the form of the local stretching force constants and their associated BSO values. However, with the introduction of ligands, the study of the aromaticity and stability of Au clusters becomes much more complicated and the relation between the cluster size/shape and the electronic structures (such as aromaticity and relative stability) is still unknown. In the current work, we carried out systematic calculations on energy gaps between frontier molecular orbitals, charge distribution, normalized atomization energy (NAE), bond strength order (BSO, n), NICS, and electron localization function (ELF)- σ of a series of $\text{Au}_m(\text{SR})_n$ clusters. It has been demonstrated that the substitution of ligands does not change much the structure of inner cores and the Au–S framework

for the studied systems [27], so the SH ligand is used for simplicity and clarity. The principal analysis (PCA) and clustering analysis were also applied to identify the important factors that governed the stability and aromaticity of $Au_m(SH)_n$ clusters. The results of energy gap, NAE and ELF- σ exhibit the odd-even effect, in which the clusters with the even number of free valence electrons, being same as the value of $(m-n)$, possess higher stability. Theoretical information may be helpful to construct the larger $Au_m(SR)_n$ clusters with reasonable stability and application potential in the future.

Computations details

All calculations were performed based on the density functional theory within Gaussian 09 program [34]. The B3LYP function was used for geometry optimizations [35,36], with the 6-31G(d,p) basis sets for nonmetal elements and LANL2DZ basis sets for gold element [37–39]. Unrestricted calculations were applied to the open-shell systems. The subsequent frequencies calculations were carried out to make sure the optimised structures were the local minima. The energetic property, NAE, magnetic property, NICS(0) (NICS values at the centroids of the rings, denoted as NICS(0)), vibrational property, bond strength order (BSO, n) and electronic density property, ELF- σ were selected to describe the stability of $Au_m(SH)_n$ clusters, same as what have done for a series of planar Au clusters in our recent work [28]. The NAE is calculated as

$$NAE = \frac{AE}{N} \quad (1)$$

where AE is the atomization energies, N is the number of total number of atoms (including Au, S, and H) in a cluster. Two different BSO equations were used since there are two kinds of bonds in the $Au_m(SH)_n$: Au–Au and Au–S (omitting the S–H bonds, as the bond length kept about 1.351 Å). To describe Au–Au and Au–S bonds, the Au–Au bonds in Au_2 and Au_3^+ , and Au–SH, Pt S were taken as reference. Meantime, the Mayer bond orders n values, with the general formula of $n = a(k^a)^b$, were 1.105, 0.610, 1.313, 2.216 for Au_2 , Au_3^+ , Au–SH and Pt S, respectively (k^a values were 1.567, 0.833, 1.806, 3.868 mdyne/Å), which gave $a = 0.724$, $b = 0.941$ for Au–Au bonds, and $a = 0.874$, $b = 0.687$ for Au–S bonds. The Au–SH, Pt = S are taken as references of the single and double bonds of Au–S, respectively. The Au = S bond does not exist from the chemical respect, so the Pt = S is taken. The single and double bonds are reflected by the Mayer bond order. The calculated bond lengths of Au–S, Pt S are 2.306, 2.087 Å, which are close to the corresponding experimental value [40–42],

although Au–SH and Pt S molecules do not exist experimentally. The atomic charges were calculated with the natural population analysis (NPA) [43]. The ELF- σ were analyzed with Multiwfn package [44]. Besides, we tried to use the multicenter index (MCI) to explain the aromaticity of these clusters. MCI, first developed by Ponec in 1997 [45], has been proven to be a useful and commonly reliable criterion to evaluate aromaticity of organic and inorganic systems [30,46–48]. However, we found it hard to define the connected order of atoms to form a ring for these three dimensional clusters, just as the chosen ring plane of the NICS(1) (calculated at 1.0 Å above the ring centroids) calculation for the three dimensional systems.

Results and discussions

Odd-even effect of the value of $(m-n)$

The initial structures of thirty $Au_m(SH)_n$ ($m, n = 5-12$) clusters were screened and sampled by the combination genetic algorithm and basin-hopping method in our previous work [27] (details in the supporting information, Figure S1), and reoptimized with B3LYP functional. Given the fact that there were no imaginary frequencies, the optimised structures were confirmed to be stable local minima. According to the topological structures of Au core and the SH ligand, we classify the studied $Au_m(SH)_n$ into four types: twisted clusters, rings attached to two central Au_3/Au_4 , interlocked clusters and other structures, as shown in Figure 1. But it will be shown that the topologically analogous clusters sometimes have quite different electronic structures.

Firstly, we compared the H-L energy gaps between the highest occupied molecular orbital (HOMO, simplified by H) and lowest unoccupied molecular orbital (LUMO, called L in short) among all the studied clusters, as listed in Figure 2(a). For the open-shell system, the H-L gap is the energy difference between the single occupied molecular orbital (SOMO- α) and the SOMO- $\alpha + 1$. An evident odd-even phenomenon was exhibited in the energy gaps of different clusters, as illustrated by the line which specifically corresponds to the clusters with even value of the difference between m and n , i.e. the $0 e^-$, $2 e^-$ and $4 e^-$ series. The value of $m-n$ also denotes the number of free valence electrons. The cluster with the even number of $m-n$ like $0 e^-$, $2 e^-$ and $4 e^-$ series does possess relatively higher energy gap than the neighbouring odd series (without the grey line in Figure 2(a)). Such an odd-even effect was also supported by some previous experimental and theoretical works where the clusters with even valence electrons exhibited higher stability and average binding energy [16,49]. During the growth process of the $Au_{25}(SR)_{18}^-$ cluster, all the stable intermediates detected

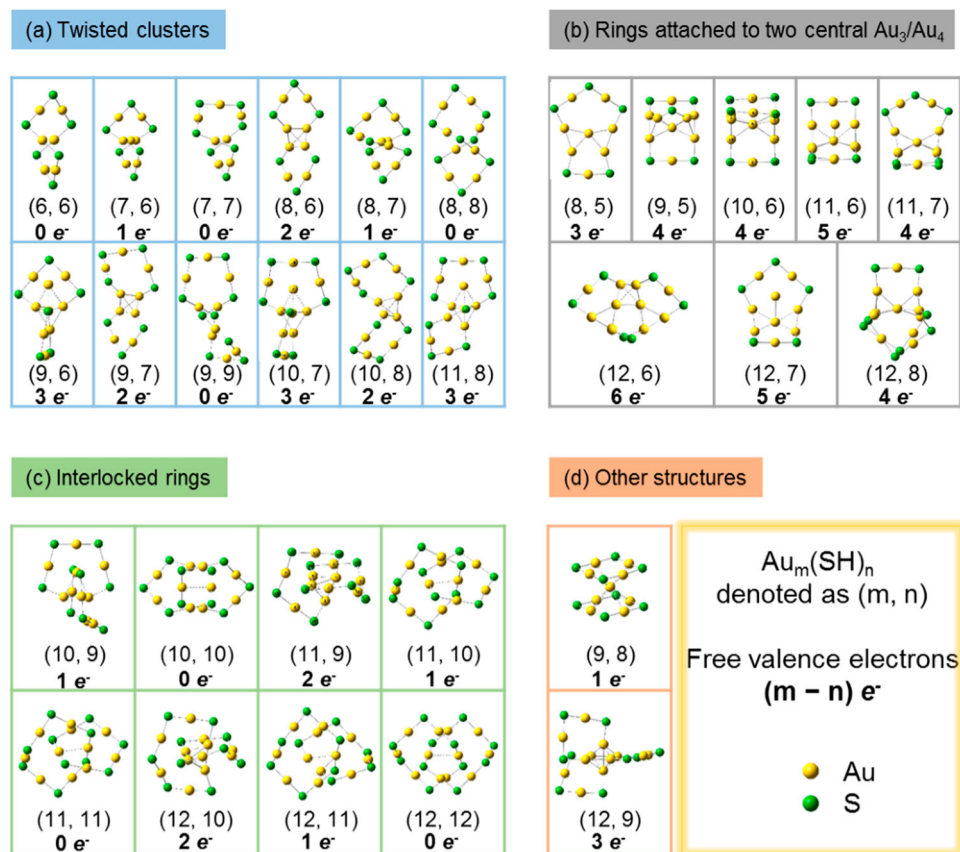


Figure 1. Four types of $Au_m(SR)_n$ ($m, n = 5-12$) clusters: (a) twisted clusters, (b) rings attached to two central Au_3/Au_4 , (c) interlocked clusters and (d) other structures. Hydrogen atoms are omitted for clarity

by the experiment were found to be the cluster with even free valence electrons from 2 to 10 [16].

How the different topologic arrangements of cluster affect the charge distribution is also worth investigating. The average charge (\bar{q}) and charge variance (Δq) of Au, S and H atoms were listed in Table 1 and Table S1, which was further analyzed with PCA analysis and shown in Table S2. The analyzed charge variance of S (Δq_s), the average charge of H (\bar{q}_H) and charge variance of H (Δq_H) are found to be quite small, so they are omitted in the following clustering analysis to avoid data redundancy. Then, the average charge of Au (\bar{q}_{Au}), the charge variance of Au (Δq_{Au}) and the average charge of S (\bar{q}_S) with the aid of K-means algorithm are used to train thirty $Au_m(SR)_n$ clusters and get one clustering model. The K-means algorithm is one of the widely used centroid-based clustering analysis methods. With this algorithm, one sample set $D = \{x_1, x_2, \dots, x_l\}$ can be divided into k ($k \leq l$) different clusters, minimising the within-cluster sum of squared criterion:

$$\min \sum_{i=1}^k \sum_{x \in C_i} \|\mu_i - x\|_2^2 \quad (2)$$

where $\mu_i = (1/|C_i|) \sum_{x \in C_i} x_i$, the mean of the C_i cluster. As illustrated in Table S3, the NPA charges are closely related with the H-L energy gaps, the value of $(m-n)$ and the existence of the Au_4 unit of clusters.

Moreover, the NAE values of $Au_m(SH)_n$ were calculated and presented in Figure 2(b). The values of all clusters are larger than the value of Au_3^+ (37.7 kcal/mol), indicating that $Au_m(SH)_n$ clusters are stable. It is worth noting that the NAE values exhibits odd-even effect similar to phenomenon in the H-L energy gaps where 2 and 4 e^- series possess relatively higher value. Therefore, the H-L energy gap and the NAE could be used as the qualitative index to measure the stability of RS-AuNPs.

Bond strength analysis

The BSO is very useful for describing the intrinsic strength of a bond in a localised chemical bonding view angle, in which the smaller BSO value indicates a weaker bond. The BSO results of all the studied systems are listed in Figure S2. The Au-S bonds with the S atom connected to Au cores are weaker than the peripheral Au-S bonds in all the selected $Au_m(SH)_n$ clusters, which is consistent

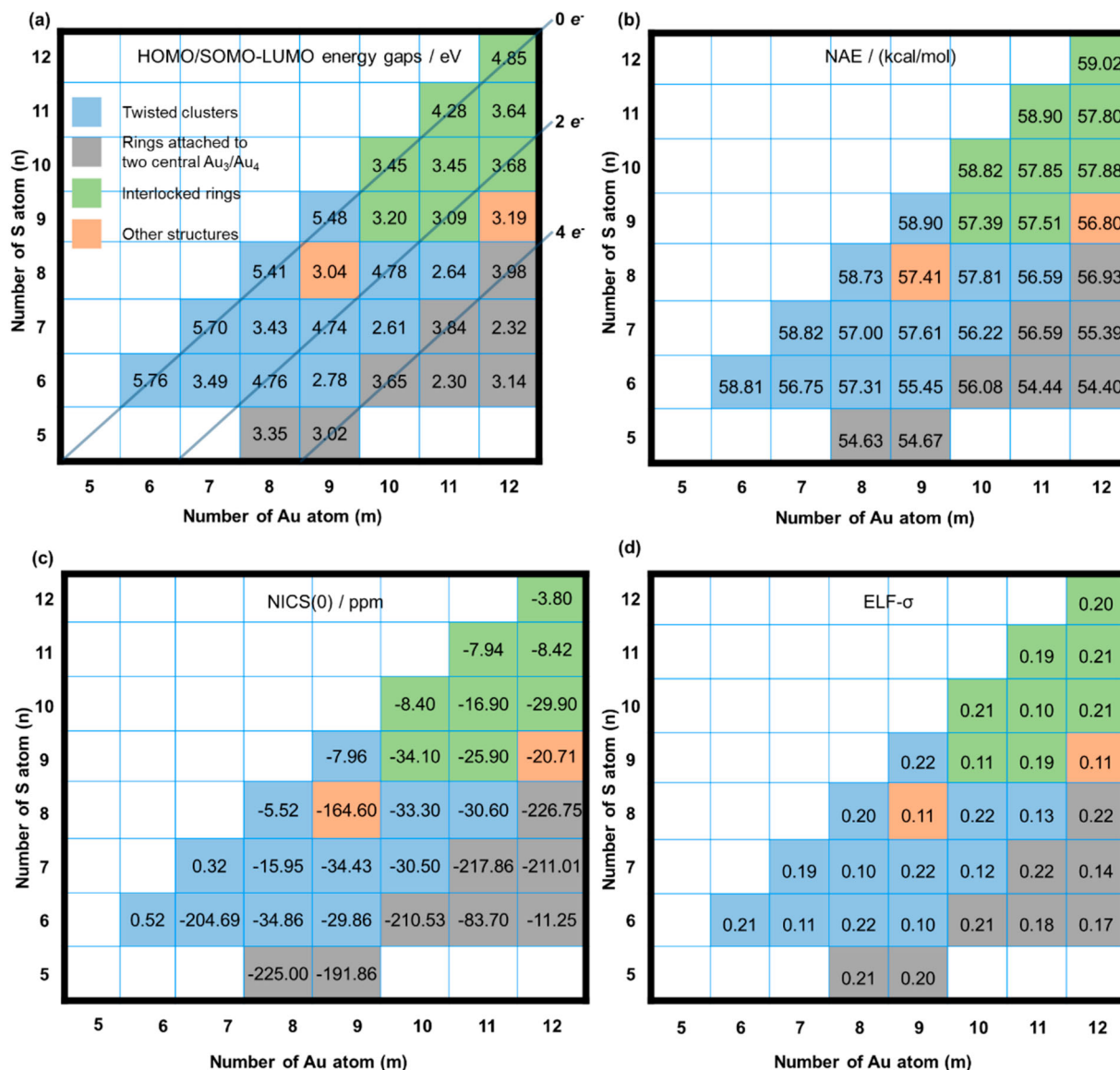


Figure 2. (a) The HOMO/SOMO-LUMO energy gaps (in eV), (b) NAE (in kcal/mol), (c), and NICS(0) (in ppm) (d) ELF- σ values of $Au_m(SR)_n$ ($m, n = 5-12$) clusters. The $0e^-$, $2e^-$, $4e^-$ means the $m-n$ values.

with what was reported for the Au–S bonds of the crystal $Au_{25}(SR)_{18}^-$ [6], as illustrated in Figure 3 and Figure S2. Most of the Au–Au bond lengths are close to the reported value (2.862 Å) in hyperconjugation favoured aromatic tetra- and octa-aurated heteroaryl complexes [50], except some ones in twisted and interlocked clusters. For $Au_m(SH)_n$ clusters with $6 \leq m = n \leq 9$, the clusters form a ring and have no Au cores, but there is a very weak Au–Au interaction in $Au_9(SR)_9$. It should be pointed out that the choice of functionals in DFT calculations is crucial to give reasonable predictions for various chemical systems, as benchmarked and discussed in literatures [51,52]. It was also mentioned that for the transition-metal containing systems the popular functional B3LYP may not be the best choice [53,54]. In

the present work, the Au–Au bond in $Au_9(SH)_9$ is aurophilic. Its bond length depends on the treatment of dispersion interactions, for which B3LYP does not perform very well. The result of the M06-2X method [55] and dispersion correction [56] show that $Au_9(SH)_9$ keeps the twisted structure (exhibited in the supporting information). The Au–Au distance changes from 3.630 Å (B3LYP) to 3.475 Å (M06-2X). There are also another two Au...Au bonds with the distances of 3.762, 3.769 Å, respectively. In $Au_7(SH)_6$ and $Au_8(SH)_7$ with odd free valence electron, the central Au atoms take part in the Au_3 core formation where Au–Au interaction is quite weak, and weaken the Au–S bonds. But for some $2e^-$ clusters, such as $Au_8(SH)_6$, $Au_9(SH)_7$ and $Au_{10}(SR)_8$, a Au_4 core lies in the cluster centre, being connected to two

Table 1. The charge data of Au and S and H atoms of $Au_m(SR)_n$ ($m, n = 5-12$).

m	n	$m-n$	$\overline{q_{Au}^a}/ e $	$\Delta q_{Au}^{2b}/ e ^2$	$\overline{q_S^c}/ e $	Energy gap ^d /eV	with or without Au ₄ ^e
6	6	0	0.2586	0.0000	-0.4538	5.76	0
7	7	0	0.2590	0.0000	-0.4550	5.7	0
8	8	0	0.2594	0.0000	-0.4543	5.41	0
9	9	0	0.2604	0.0002	-0.4571	5.48	0
10	10	0	0.2427	0.0171	-0.4373	3.45	0
11	11	0	0.2442	0.0135	-0.4390	4.28	0
12	12	0	0.2475	0.0081	-0.4423	4.85	0
7	6	1	0.1841	0.0253	-0.4097	3.49	0
8	7	1	0.1901	0.0316	-0.4123	3.43	0
9	8	1	0.2023	0.0548	-0.4210	3.04	0
10	9	1	0.1994	0.0305	-0.4143	3.2	0
11	10	1	0.2140	0.0248	-0.4298	3.45	0
12	11	1	0.2215	0.0160	-0.4362	3.64	0
8	6	2	0.1858	0.0067	-0.4428	4.76	1
9	7	2	0.1971	0.0062	-0.4484	4.74	1
10	8	2	0.2078	0.0064	-0.4543	4.78	1
11	9	2	0.1963	0.0372	-0.4323	3.09	1
12	10	2	0.2066	0.0349	-0.4430	3.68	1
8	5	3	0.1500	0.0113	-0.4337	3.35	0
9	6	3	0.1518	0.0110	-0.4232	2.78	1
10	7	3	0.1602	0.0003	-0.4240	2.61	1
11	8	3	0.1727	0.0162	-0.4328	2.64	1
12	9	3	0.1846	0.0218	-0.4411	3.19	0
9	5	4	0.1518	0.0149	-0.4665	3.02	1
10	6	4	0.1581	0.0178	-0.4576	3.65	1
11	7	4	0.1640	0.0145	-0.4518	3.84	1
12	8	4	0.1702	0.0147	-0.4497	3.98	1
11	6	5	0.1369	0.0335	-0.4446	2.3	1
12	7	5	0.1399	0.0289	-0.4347	2.32	1
12	6	6	0.1370	0.0162	-0.4669	3.14	1

^aThe average charge of Au.^bThe charge variance of Au is calculated as $\sum (q_{Au}^i - \overline{q_{Au}})^2/m$, where q_{Au}^i is the charge of the i th Au.^cThe average charge of S.^dThe energy gap between the HOMO (or SOMO- α) and the LUMO (SOMO- $\alpha + 1$).^eIf there is Au₄ unit in clusters, the value is '1'. Otherwise, the value is '0'.

peripheral rings. For $Au_9(SR)_7$, the Au–S bonds in the larger ring are slightly stronger due to less strain which does not happen in $Au_8(SH)_6$ or $Au_{10}(SH)_8$ because they have two similar 7- or 9-membered rings. The Au₅ core in $3e^- Au_9(SH)_6$, $Au_{10}(SH)_7$ and $Au_{11}(SH)_8$ can be viewed as a trigonal bipyramid formed by two Au₄ sharing a plane. In $Au_9(SH)_6$, the 2# Au (on top of the ring) of the Au₅ core forms weak Au–Au interactions via the long bond distance, and weaken Au–S bonds of the 7-membered ring (Figure 3). The larger 9-membered ring in $Au_{10}(SH)_7$ can accommodate the 2# Au better (closer to planar), when compared to $Au_9(SH)_6$ cluster. The Au–Au interactions with 2# Au tend to be stronger. The $Au_{11}(SH)_8$ cluster has two 9-membered ring, one of which is with an Au on top of the ring. Meanwhile, the BSO values of the Au–Au and Au–S bonds in the ring which accommodates one Au atom belonging to the Au₅ cores in $Au_9(SH)_6$, $Au_{10}(SH)_7$ and $Au_{11}(SH)_8$ are smaller than those in the ring with the same size in $Au_8(SH)_6$, $Au_9(SH)_7$ and $Au_{10}(SH)_8$.

The small number of SH groups (starting from $n = 5$) contributes to the formation of bigger Au clusters in the centre of the structure, and those Au cores share the connected apex. As shown in Figure 3 and Figure S2, the $Au_8(SH)_5$ contains two Au₃; the $Au_9(SH)_5$, $Au_{10}(SH)_6$, $Au_{11}(SH)_7$ and $Au_{12}(SH)_8$ have two Au₄ cores; the $Au_{11}(SH)_6$ and $Au_{12}(SH)_7$ also possess two Au₄ cores, and also an extra Au atom; the $Au_{12}(SH)_6$ have three Au₄ cores. The five central Au atoms in the $Au_8(SH)_5$ do not form a trigonal bipyramid like those in the $Au_9(SH)_6$, $Au_{10}(SH)_7$ and $Au_{11}(SH)_8$, but its Au–Au interaction ($n = 0.528-0.573$) is the strongest. The central gold atom of the $Au_9(SH)_5$ leads to the formation of two 6-membered rings and a 4-membered ring connected to two central tetrahedral. The strain in the 4-membered ring results in weaker Au–S bonds. With an extra Au–SH, the $Au_{10}(SH)_6$ cluster has three 6-membered rings attached to the two tetrahedral, the Au–Au interactions are stronger due to the smaller strain of the 6-membered ring when compared to the 4-membered ring in the $Au_9(SH)_5$. The $Au_{11}(SH)_7$ and $Au_{12}(SH)_8$ clusters are comparable to $Au_{10}(SH)_6$, where the extra Au–SR leads to an expanded ring. The Au–S interactions (except those connected to the Au₇ cores) in the 8-membered rings of the $Au_{11}(SH)_7$ and $Au_{12}(SH)_8$ are stronger than those in the 6-membered rings of the $Au_9(SH)_5$ and $Au_{10}(SH)_6$. The $Au_{12}(SH)_6$ has the largest $m-n$ value, 6, and the largest Au core containing three distorted tetrahedrons. The weakest Au–Au bonds are those containing the shared apexes among the Au cores of the rings attached to two central Au₃/Au₄.

Large clusters with a similar number of Au and SH units tend to form interlocked rings. There are three different types of Au cores in these clusters: the Au₂ cores in the $Au_{10}(SH)_{10}$, $Au_{11}(SH)_{11}$ and $Au_{12}(SH)_{12}$; the Au₃ cores in the $Au_{10}(SH)_9$, $Au_{11}(SH)_{10}$, $Au_{12}(SH)_{11}$; the Au₄ cores in the $Au_{11}(SH)_9$ and $Au_{12}(SH)_{10}$. As we mentioned before, the increasing number of Au atoms promotes to form the large Au cores, so called the core nucleation [27]. From $Au_{10}(SH)_{10}$ to $Au_{12}(SH)_{12}$, the bond lengths and n values of the Au₂ cores increase, while those of the Au–S related to the Au₂ cores decrease. It can be seen from Figure 3 that the two Au atoms of the Au₂ cores stay far away from each other, so the two interlocked rings behave similarly to twisted clusters due to weak interactions in $Au_{12}(SH)_{12}$. In the Au₃ core of the $Au_{10}(SH)_9$, the two Au atoms of the 9-membered ring form strong Au–Au interaction, but they interact weakly with another Au atom belonging to the 10-membered ring. This also happens in the Au₃ cores of $Au_{11}(SH)_{10}$ and $Au_{12}(SH)_{11}$. The Au–Au interactions in the Au₄ core of the $Au_{11}(SH)_9$, $Au_{12}(SH)_{10}$ are comparable to those of the rings attached to two Au₄.

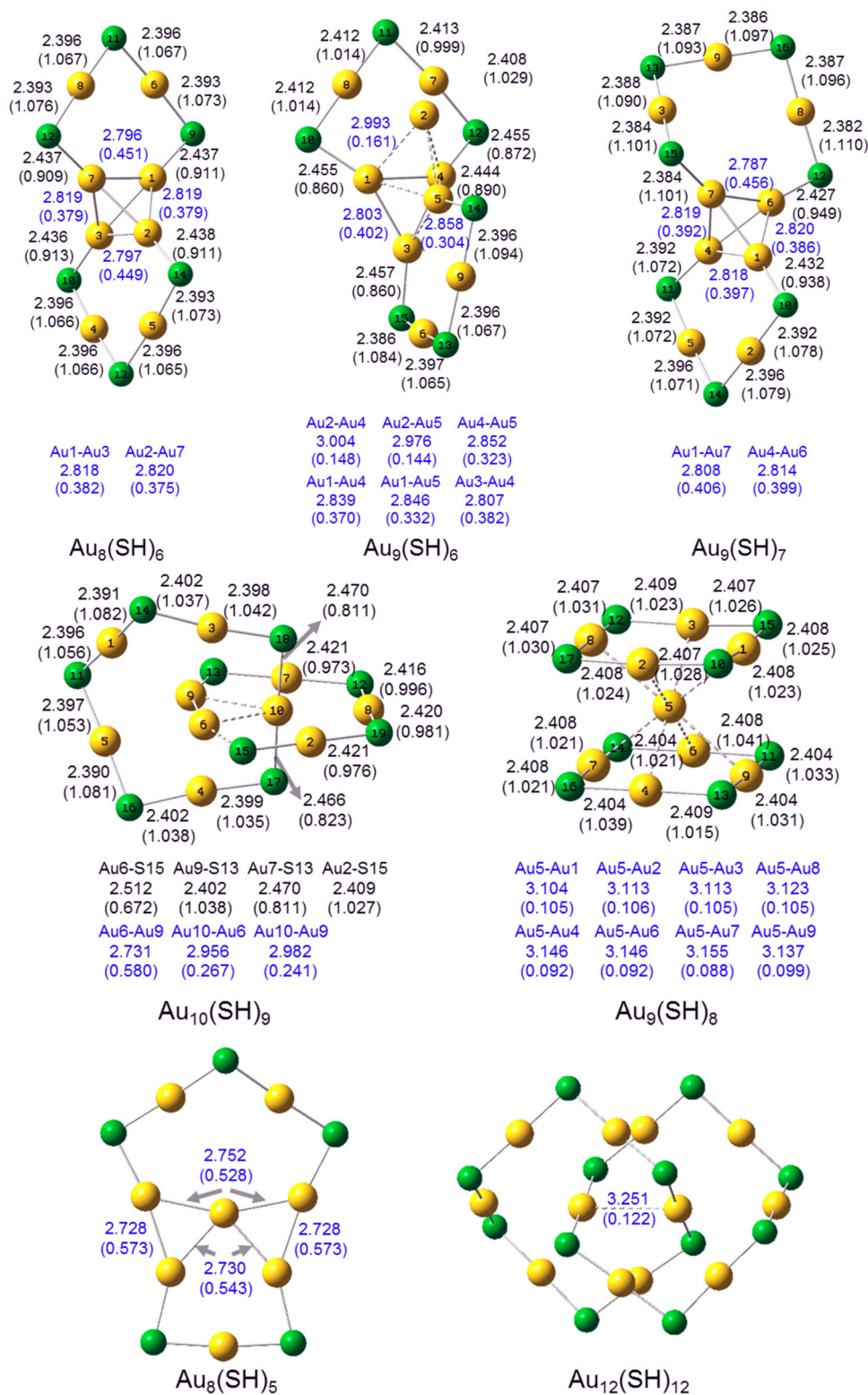


Figure 3. The bond length (Å, black) and bond strength order (arbitrary unit, blue, in parenthesis) of the Au–S and Au–Au in some selected $Au_m(SH)_n$ clusters. The strongest and weakest Au–Au bonds in the Au_5 cores of the $Au_8(SR)_5$ cluster, and the Au_2 cores of the $Au_{12}(SR)_{12}$ cluster are also shown.

The $Au_9(SH)_8$ and $Au_{12}(SH)_9$ clusters behave differently compared to the above-mentioned clusters. The $Au_9(SH)_8$ contains two stacked 8 membered rings with

a Au atom in the centre. The central Au atom forms quite weak interactions with other Au atoms. The Au_6 cores of the $Au_{12}(SH)_9$ can be understood as an octahedron or a

combination of two Au₄. The Au–Au bonds which connect three SH ligands are stronger than the other Au–Au bonds.

In summary, some trends appear from the BSO analysis: (i) The Au–S bonds become weaker when connected to the Au cores, which can be used to figure out the Au core of the Au_m(SH)_n clusters. (ii) The peripheral Au–Au bonds of the Au cores linking the SH ligands are stronger compared to the inner ones. (iii) The strongest Au–Au bonds ($n = 0.573$) belong to the Au₅ cores of the Au₈(SH)₅ cluster, and the weakest Au–Au bonds ($n = 0.051$) belong to the Au₂ cores of the Au₁₂(SH)₁₂ cluster (Figure 3). (iv) The Au_m(SH)_n clusters with the same Au cores, i.e. the same $m-n$ values (also the number of free valence electrons), exhibit some similarities. This is in agreement with the odd-even effect revealed from the H-L gaps and other aromaticity index, as shown in Figure 2.

Aromaticity

We also try to analyze the aromaticity of the Au_m(SH)_n clusters from two aromaticity indexes, NICS and ELF- σ . The NICS(0) and ELF- σ values of Au_m(SH)_n clusters ($m, n = 5-12$) are listed in Figure 2 (c) and (d). The reported σ -aromatic Au₅Zn⁺ system is chosen as a reference [57]. Recently, the concept of σ -aromaticity has been investigated both experimentally and theoretically and extended to unsaturated systems [58–60]. The NICS(0) and ELF- σ values of Au₅Zn⁺ are -23.97 ppm and 0.18 at the same calculation level, respectively. For the NICS(0) analysis, which is an evaluation based on the planar ring electricity, there is no evident trend, probably due to the limitation of application of NICS(0) in the sophisticated three dimensional clusters. The value of ELF- σ is controlled by the contributions of σ orbitals and calculated at the bifurcation point of two ELF domains, which is in the range of $0-1$ [61]. It reveals the degree of interaction between adjacent ELF domains: A larger ELF- σ value indicates that the electrons are more strongly delocalised between adjacent domains. ELF- σ method, on the other hand, shows a similar odd-even effect that the clusters with even valence electrons have higher value and stability. Hence, the local parameters such as BSO and ELF- σ could be a useful tool to evaluate the stability of the complicated RS-AuNPs.

Conclusions

With different arrangements of Au–SR rings, the Au_m(SH)_n ($m, n = 5-12$) clusters are classified into four types: twisted clusters, rings attached to two central Au₃/Au₄, interlocked clusters and other structures. Their

electronic structures were investigated from energetic, vibrational, magnetic and electronic density aspects. An evident odd-even dependence of the number of free valence electrons was observed in this work. The H-L gaps, NAE values and ELF- σ methods all pointed out that the cluster with even number of free valence electrons possess higher stability than the odd ones. The principal component analysis of the NPA charge and clustering analysis showed that there is obvious change on the charge distributions of Au and S atoms in different sized clusters. Through the BSO evaluation, the detailed geometrical parameters were found to be sensitive to the value of $(m-n)$. The Au_m(SH)_n clusters with the same $(m-n)$ values exhibited some similarities in bond strength distribution. The Au–S bonds connected to the Au cores become weaker, which can be used to distinguish Au atoms in the ligands or cores. The aromatic index of NICS(0) is not applicable to the complex geometric structures of Au_m(SH)_n clusters. More efficient chemical bond models are still desired to derive the structure and stability relationship of the three dimensional cluster structures.

Acknowledgements

We are grateful to the High Performance Computing Centre of Nanjing University for providing the IBM Blade cluster system.

Disclosure statement

No potential conflict of interest was reported by the authors.

Funding

This work was supported by the National Key Research and Development Program of China under [grant number 2017YFB0702600, 2017YFB0702601] and the National Natural Science Foundation of China under [grant number No. 21673111].

References

- [1] H. Masatake, K. Tetsuhiko, S. Hiroshi and Y. Nobumasa, Chem. Lett. **16** (2), 405 (1987).
- [2] Y. Zhu, H. Qian, M. Zhu and R. Jin, Adv. Mater. **22** (17), 1915 (2010).
- [3] G. Li, D.-e. Jiang, S. Kumar, Y. Chen and R. Jin, ACS Catal. **4** (8), 2463 (2014).
- [4] O.A. Wong, R.J. Hansen, T.W. Ni, C.L. Heinecke, W.S. Compel, D.L. Gustafson and C.J. Ackerson, Nanoscale. **5** (21), 10525 (2013).
- [5] M. Wang, Z. Wu, J. Yang, G. Wang, H. Wang and W. Cai, Nanoscale. **4** (14), 4087 (2012).
- [6] M. Zhu, C.M. Aikens, F.J. Hollander, G.C. Schatz and R. Jin, J. Am. Chem. Soc. **130** (18), 5883 (2008).
- [7] A. Das, T. Li, G. Li, K. Nobusada, C. Zeng, N.L. Rosi and R. Jin, Nanoscale. **6** (12), 6458 (2014).

- [8] H. Qian, W.T. Eckenhoff, Y. Zhu, T. Pintauer and R. Jin, *J. Am. Chem. Soc.* **132** (24), 8280 (2010).
- [9] D. Crasto, S. Malola, G. Brosofsky, A. Dass and H. Häkkinen, *J. Am. Chem. Soc.* **136** (13), 5000 (2014).
- [10] G. Li and R. Jin, *Acc. Chem. Res.* **46** (8), 1749 (2013).
- [11] H. Grönbeck, M. Walter and H. Häkkinen, *J. Am. Chem. Soc.* **128** (31), 10268 (2006).
- [12] N. Shao, Y. Pei, Y. Gao and X.C. Zeng, *J. Phys. Chem. A.* **113** (4), 629 (2009).
- [13] K.A. Kacprzak, O. Lopez-Acevedo, H. Häkkinen and H. Grönbeck, *J. Phys. Chem. C.* **114** (32), 13571 (2010).
- [14] B.M. Barngrover and C.M. Aikens, *J. Phys. Chem. A.* **115** (42), 11818 (2011).
- [15] B.M. Barngrover and C.M. Aikens, *J. Phys. Chem. Lett.* **2** (9), 990 (2011).
- [16] Z. Luo, V. Nachammai, B. Zhang, N. Yan, D.T. Leong, D.-e. Jiang and J. Xie, *J. Am. Chem. Soc.* **136** (30), 10577 (2014).
- [17] F. Bertorelle, I. Russier-Antoine, N. Calin, C. Comby-Zerbino, A. Bensalah-Ledoux, S. Guy, P. Dugourd, P.-F. Brevet, Ž Sanader, M. Krstić, V. Bonačić-Koutecký and R. Antoine, *J. Phys. Chem. Lett.* **8** (9), 1979 (2017).
- [18] D.-e. Jiang, S.H. Overbury and S. Dai, *J. Am. Chem. Soc.* **135** (24), 8786 (2013).
- [19] L. Gell, A. Kulesza, J. Petersen, M.I.S. Röhr, R. Mitrić and V. Bonačić-Koutecký, *J. Phys. Chem. C.* **117** (28), 14824 (2013).
- [20] Y. Pei, Y. Gao and X.C. Zeng, *J. Am. Chem. Soc.* **130** (25), 7830 (2008).
- [21] H. Häkkinen, M. Walter and H. Grönbeck, *J. Phys. Chem. B.* **110** (20), 9927 (2006).
- [22] P.D. Jadzinsky, G. Calero, C.J. Ackerson, D.A. Bushnell and R.D. Kornberg, *Science*. **318** (5849), 430 (2007).
- [23] M. Walter, J. Akola, O. Lopez-Acevedo, P.D. Jadzinsky, G. Calero, C.J. Ackerson, R.L. Whetten, H. Grönbeck and H. Häkkinen, *Proc. Natl. Acad. Sci. USA.* **105** (27), 9157 (2008).
- [24] L. Cheng, C. Ren, X. Zhang and J. Yang, *Nanoscale.* **5** (4), 1475 (2013).
- [25] L. Cheng, Y. Yuan, X. Zhang and J. Yang, *Angew. Chem. Int. Ed.* **52** (34), 9035 (2013).
- [26] W.W. Xu, B. Zhu, X.C. Zeng and Y. Gao, *Nat. Commun.* **7** (2016).
- [27] C. Liu, Y. Pei, H. Sun and J. Ma, *J. Am. Chem. Soc.* **137** (50), 15809 (2015).
- [28] Y. Li, V. Oliveira, C. Tang, D. Cremer, C. Liu and J. Ma, *Inorg. Chem.* **56** (10), 5793 (2017).
- [29] E. Clar and R. Schoental, eds. *Book Polycyclic Hydrocarbons* (Springer, 1964).
- [30] J. Wu and J. Zhu, *Chem. Phys. Chem.* **16** (18), 3806 (2015).
- [31] Z. Konkoli and D. Cremer, *Int. J. Quantum Chem.* **67** (1), 1 (1998).
- [32] W. Zou, R. Kalescky, E. Kraka and D. Cremer, *J. Chem. Phys.* **137** (8), 084114 (2012).
- [33] W. Zou and D. Cremer, *Theor. Chem. Acc.* **133** (3), 1 (2014).
- [34] M. Frisch, G. Trucks, H. Schlegel, G. Scuseria, M. Robb, J. Cheeseman, G. Scalmani, V. Barone, B. Mennucci and G. Petersson, *Gaussian09*, Revision D01.
- [35] A.D. Becke, *J. Chem. Phys.* **98** (7), 5648 (1993).
- [36] C. Lee, W. Yang and R.G. Parr, *Phys. Rev. B.* **37** (2), 785 (1988).
- [37] P.J. Hay and W.R. Wadt, *J. Chem. Phys.* **82** (1), 270 (1985).
- [38] W.R. Wadt and P.J. Hay, *J. Chem. Phys.* **82** (1), 284 (1985).
- [39] P.J. Hay and W.R. Wadt, *J. Chem. Phys.* **82** (1), 299 (1985).
- [40] R. Jones, D.J. Williams, P.T. Wood and J.D. Woollins, *Polyhedron.* **6** (3), 539 (1987).
- [41] J.C. Poat, A.M.Z. Slawin, D.J. Williams and J.D. Woollins, *J. Chem. Soc., Chem. Commun.* **0** (15), 1036 (1990).
- [42] T.S. Lobana, R. Verma and A. Castineiras, *Polyhedron.* **17** (21), 3753 (1998).
- [43] F. Weinhold and C.R. Landis, eds. *Book Valency and Bonding: A Natural Bond Orbital Donor-Acceptor Perspective* (Cambridge University Press, Cambridge, 2005).
- [44] L. Tian and C. Feiwu, *J. Comput. Chem.* **33** (5), 580 (2012).
- [45] R. Ponec and I. Mayer, *J. Phys. Chem. A.* **101** (9), 1738 (1997).
- [46] M. Giambiagi, M.S. de Giambiagi, C.D. dos Santos Silva and A.P. de Figueiredo, *Phys. Chem. Chem. Phys.* **2** (15), 3381 (2000).
- [47] N. Otero, S. Fias, S. Radenković, P. Bultinck, A.M. Graña and M. Mandado, *Chem. - Eur. J.* **17** (11), 3274 (2011).
- [48] Q. Xie, T. Sun and J. Zhu, *Organometallics.* **37** (18), 3219 (2018).
- [49] Y. Yu, Z. Luo, Y. Yu, J.Y. Lee and J. Xie, *ACS Nano.* **6** (9), 7920 (2012).
- [50] J. Yuan, T. Sun, X. He, K. An, J. Zhu and L. Zhao, *Nat. Commun.* **7**, 11489 (2016).
- [51] N. Mardirossian and M. Head-Gordon, *Mol. Phys.* **115** (19), 2315 (2017).
- [52] L. Goerigk, A. Hansen, C. Bauer, S. Ehrlich, A. Najibi and S. Grimme, *Phys. Chem. Chem. Phys.* **19** (48), 32184 (2017).
- [53] T. Weymuth, E.P.A. Couzijn, P. Chen and M. Reiher, *J. Chem. Theory Comput.* **10** (8), 3092 (2014).
- [54] S. Dohm, A. Hansen, M. Steinmetz, S. Grimme and M.P. Checinski, *J. Chem. Theory Comput.* **14** (5), 2596 (2018).
- [55] Y. Zhao and D.G. Truhlar, *Theor. Chem. Acc.* **120** (1-3), 215 (2008).
- [56] S. Grimme, J. Antony, S. Ehrlich and H. Krieg, *J. Chem. Phys.* **132** (15), 154104 (2010).
- [57] H. Tanaka, S. Neukermans, E. Janssens, R.E. Silverans and P. Lievens, *J. Am. Chem. Soc.* **125** (10), 2862 (2003).
- [58] C. Zhu, X. Zhou, H. Xing, K. An, J. Zhu and H. Xia, *Angew. Chem. Int. Ed.* **54** (10), 3102 (2015).
- [59] Y. Hao, J. Wu and J. Zhu, *Chem. - Eur. J.* **21** (51), 18805 (2015).
- [60] X. Zhou, J. Wu, Y. Hao, C. Zhu, Q. Zhuo, H. Xia and J. Zhu, *Chem. - Eur. J.* **24** (10), 2389 (2018).
- [61] J. Santos, W. Tiznado, R. Contreras and P. Fuentealba, *J. Chem. Phys.* **120** (4), 1670 (2004).